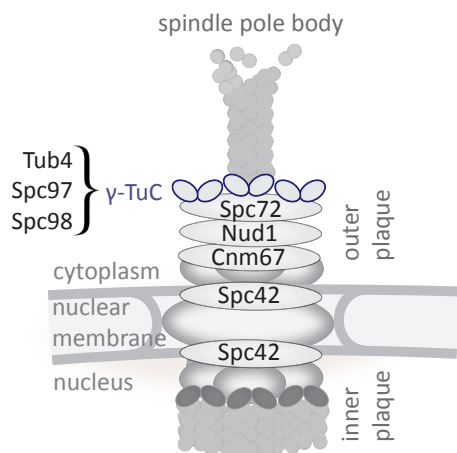
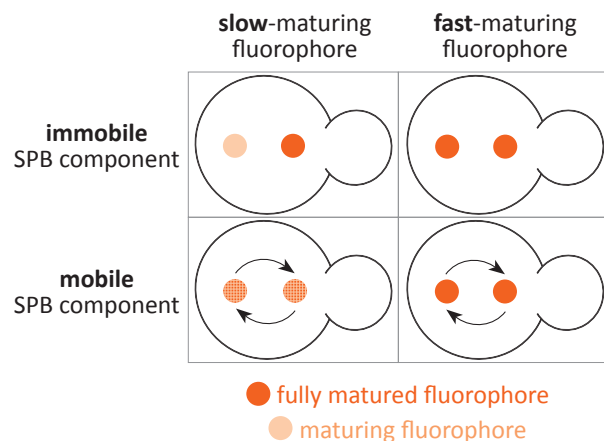
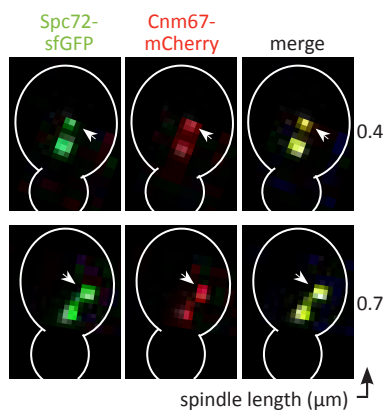
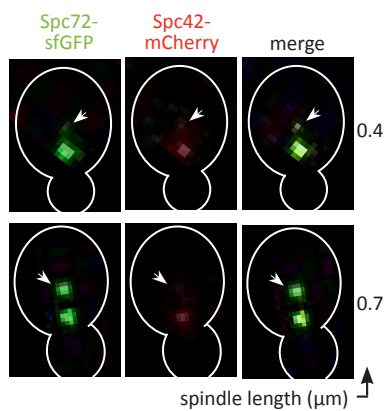
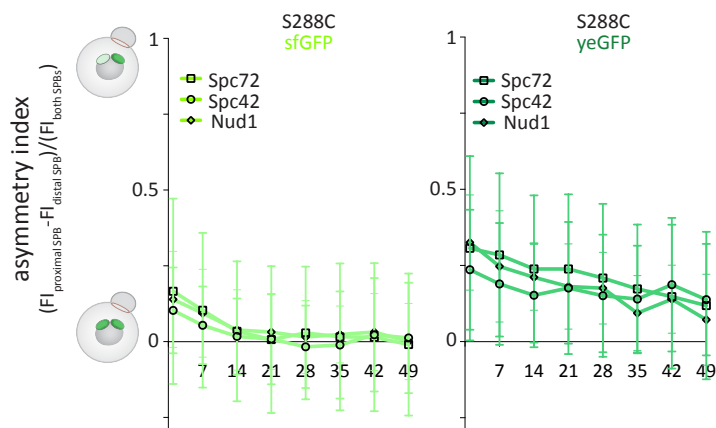
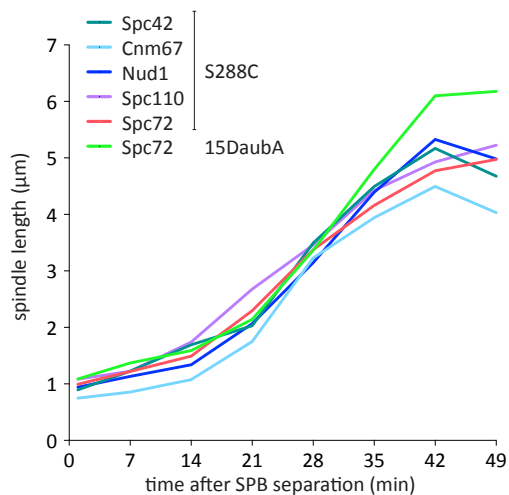


# Supplemental Materials

*Molecular Biology of the Cell*

Lengefeld et al.

**A****B****C****D****E**

**FIGURE S1: Analysis of outer plaque assembly kinetics.**

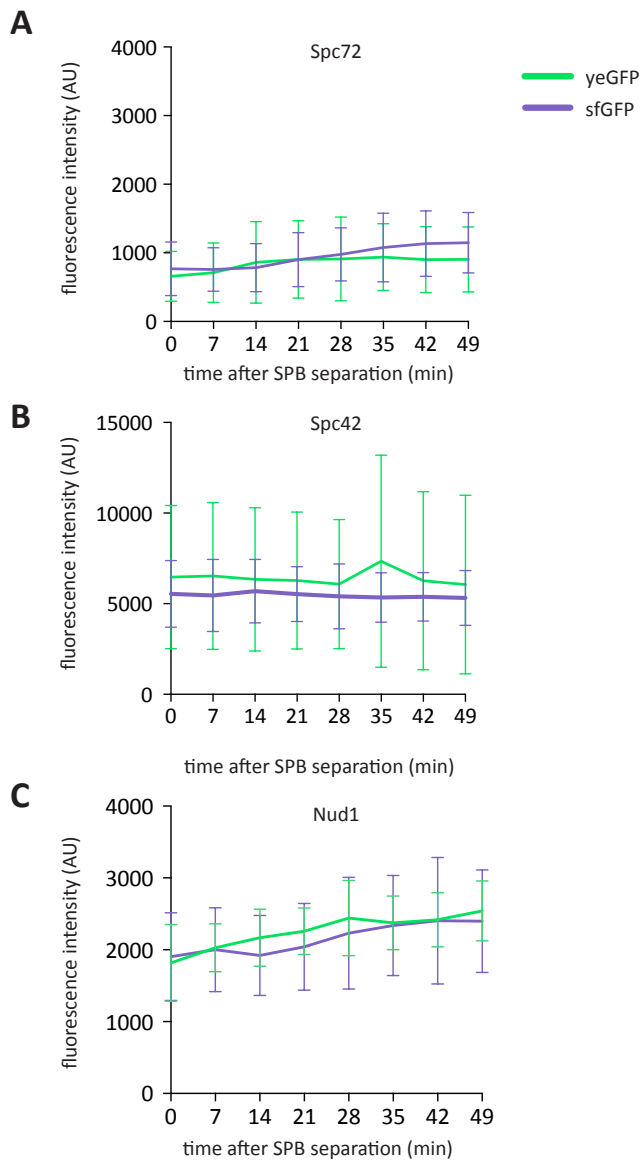
(A) Schematic representation of the rationale of fluorophore usage with different maturation time.

(B) Schematic representation of the spindle pole body. Adapted from (Jaspersen and Winey, 2004).

(C) Representative images of Spc72-sfGFP asymmetry in combination with Spc42-mCherry and Cnm67-mCherry at indicated spindle length ( $\mu\text{m}$ ).

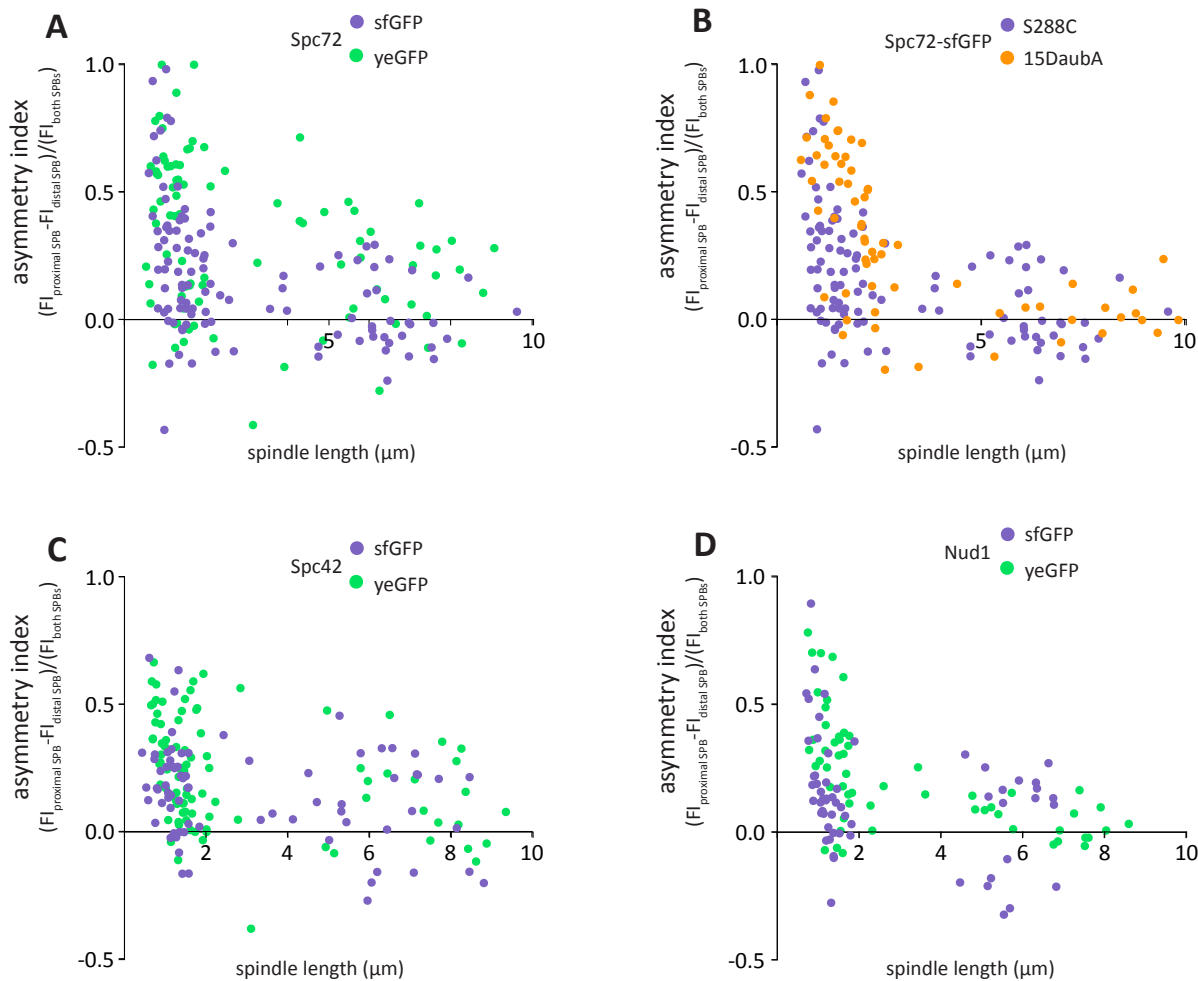
(D) Comparison of sfGFP and yeGFP tagged to Spc72, Spc42 and Nud1. Raw data as in figure 2B.

(E) Quantification and comparison of spindle length ( $\mu\text{m}$ ) of SPB components tagged with sfGFP (n = 50 cells analyzed at each time point from three independent experiments, mean).



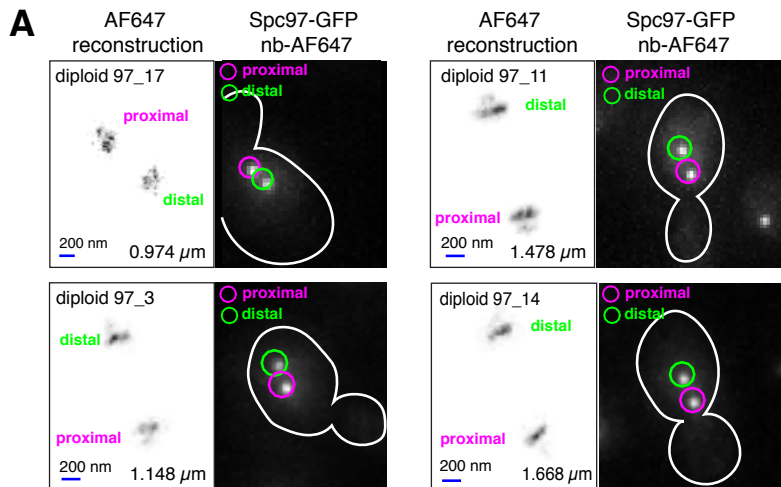
**FIGURE S2: Analysis of outer plaque assembly kinetics.**

Fluorescence intensity (AU) of (A) Spc72, (B) Spc42, (C) Nud1 tagged with sfGFP or yeGFP at the pre-existing SPB over time (min) ( $n = 60$  cells analyzed at each time point from three independent experiments, mean  $\pm$  SD). All panels: Raw data as in Figure 2.



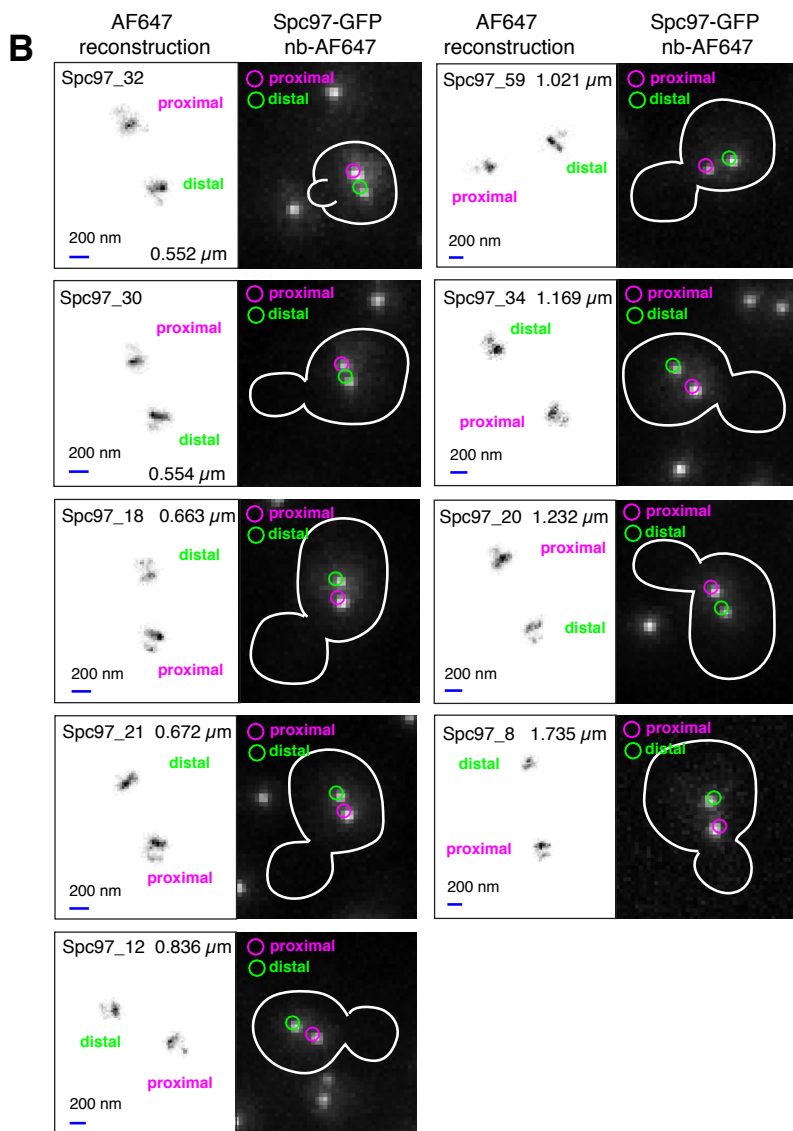
**FIGURE S3: Analysis of outer plaque assembly kinetics.**

Asymmetry index of (A) Spc72-yeGFP ( $n = 117$ ) and Spc72-sfGFP ( $n = 111$ ), (B) Spc72-sfGFP in S288C ( $n = 111$ ) and 15DaubA ( $n = 63$ ), (C) Spc42-yeGFP ( $n = 90$ ) and Spc42-sfGFP ( $n = 61$ ), (D) Nud1-yeGFP ( $n = 63$ ) and Nud1-sfGFP ( $n = 71$ ) plotted versus spindles length ( $\mu\text{m}$ ).  $n =$  cells measured from three independent experiments.



**FIGURE S4: Proximal- and distal-plaques contain at least one complete  $\gamma$ -TuC complex.**

Representative images (confocal, distribution of localization events and reconstruction) of SPBs in fixed (A) diploid and (B) haploid cell, with Spc72-GFP labeled with nb-AF647. Sample name and spindle length is provided in the confocal image. Bar in reconstruction is 200 nm.



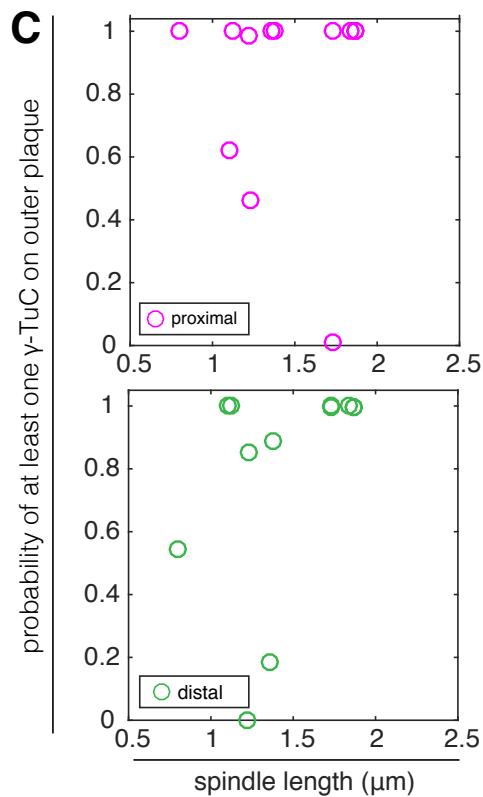
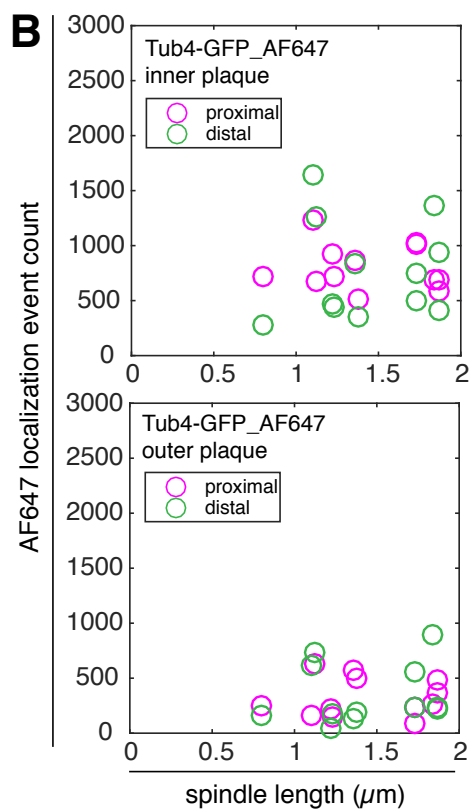
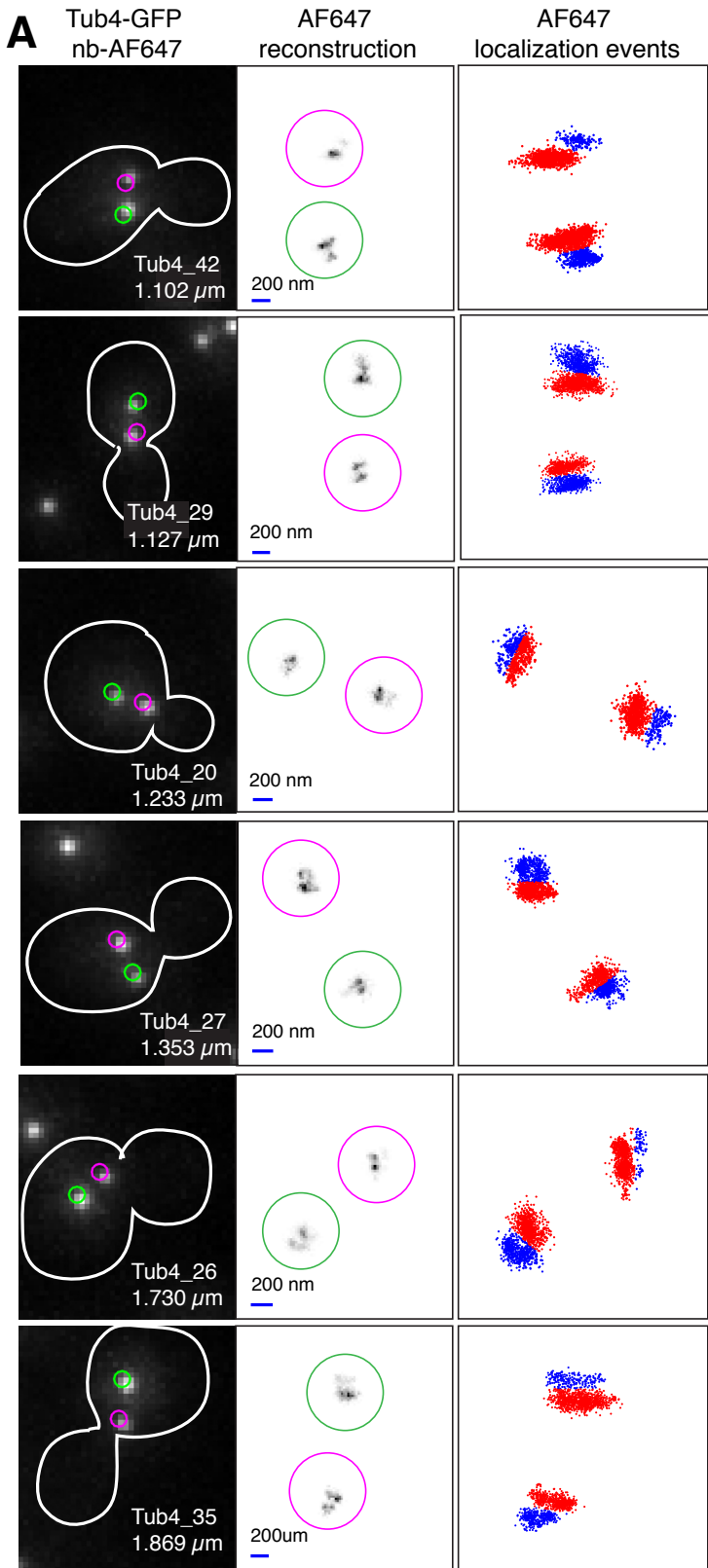


**FIGURE S5: Proximal- and distal- plaques contain at least one complete  $\gamma$ -TuC complex.**

(A) Representative images (confocal, distribution of localization events and reconstruction) of SPBs in fixed cells, with Tub4-GFP labeled with nb-AF647. Sample name and spindle length is provided in the confocal image. Bar in reconstruction is 200 nm.

(B) Number of localization events for Tub4-GFP-AF647 on the inner and outer plaques.

(C) Probability of having at least one complete  $\gamma$ -TuC on the outer plaques of both SPBs.

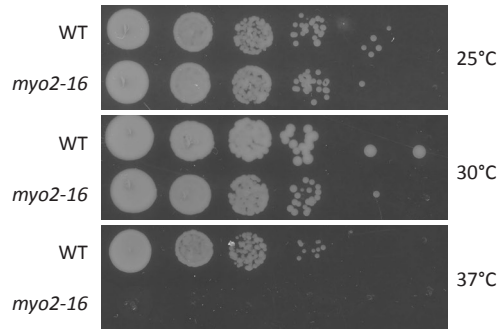


**FIGURE S6: The *myo2-16* mutation does not display growth defects at 30°C.**

(A) Comparison of growth between wild type and *myo2-16* mutant cells. Serial dilutions of stationary phase cultures of the indicate strains were spotted on YPD plates and incubated at 25°C, 30°C or 37°C.

## Supplemental Tables

**Table S1: Strain list**

<b>S288C</b>
<i>SPC72-sfGFP:KanMX4, swe1::hphNT1</i>
<i>SPC72-sfGFP:KanMX4, yaf9::hphNT1</i>
<i>SPC72-sfGFP:KanMX4, kin3::hphNT1</i>
<i>SPC72-sfGFP:KanMX4, tem1-3</i>
<i>SPC72-sfGFP:KanMX4, cdc15-1</i>
<i>SPC72-sfGFP:KanMX4, myo2-16</i>
<i>SPC72-sfGFP:KanMX4, kar9::KanMX4</i>
<i>SPC72-yeGFP:hphNT1, swe1::hphNT1</i>
<i>SPC72-yeGFP:hphNT1, yaf9::hphNT1</i>
<i>SPC72-yeGFP:hphNT1, kin3::hphNT1</i>
<i>SPC72-yeGFP:hphNT1, tem1-3</i>
<i>SPC72-yeGFP:hphNT1, cdc15-1</i>
<i>SPC72-yeGFP:hphNT1, myo2-16</i>
<i>SPC72-yeGFP:hphNT1, kar9::KanMX4</i>
<i>SPC72-sfGFP:KanMX4</i>
<i>SPC72-yeGFP:hphNT1</i>
<i>SPC72-mCherry:KanMX4</i>
<i>NUD1-sfGFP:KanMX4</i>
<i>NUD1-yeGFP:hphNT1</i>
<i>NUD1-mCherry:KanMX4</i>
<i>CNM67-3xsfGFP:KanMX4</i>
<i>CNM67-yeGFP:hphNT1</i>
<i>CNM67-mCherry:KanMX4</i>
<i>SPC42-sfGFP:KanMX4</i>
<i>SPC42-yeGFP:HIS3MX6</i>
<i>SPC42-mCherry:NatNT2</i>
<i>SPC110-sfGFP:KanMX4</i>
<i>SPC110-yeGFP:hphNT1</i>
<i>SPC110-mCherry:KanMX4</i>
<i>SPC72-sfGFP:KanMX4, SPC42-mCherry:NatNT2</i>
<i>SPC72-sfGFP:KanMX4, CNM67-mCherry:KanMX4</i>
<i>SPC42-mCherry:KanMX4, ura3::CFP-TUB1:URA3</i>
<i>swe1::hphNT1, SPC42-mCherry:KanMX4, ura3::CFP-TUB1:URA3</i>
<i>kin3::hphNT1, SPC42-mCherry:KanMX4, ura3::CFP-TUB1:URA3</i>
<i>yaf9::hphNT1, SPC42-mCherry:KanMX4, ura3::CFP-TUB1:URA3</i>
<i>SPC72-loxPmCherry:KanMX4loxP:GFP:HIS3MX6, ura3::CFP-TUB1:URA3, leu2::GDP:creEBD78:LEU2</i>
<i>CNM67-loxPmCherry:KanMX4loxP:GFP:HIS3MX6, ura3::CFP-TUB1:URA3, leu2::GDP:creEBD78:LEU2</i>
<i>SPC42-loxPmCherry:KanMX4loxP:GFP:HIS3MX6, ura3::CFP-TUB1:URA3, leu2::GDP:creEBD78:LEU2</i>
<i>SPC97-GFP::HIS3MX6</i>
<i>TUB4-GFP::HIS3MX6</i>
<i>SPC42-mCherry:KanMX4, ura3::CFP-TUB1:URA3, KAR9-YFP:NatNT2</i>
<i>SPC42-mCherry:KanMX4, ura3::CFP-TUB1:URA3, KAR9-YFP:NatNT2, myo2-16</i>
<i>SPC42-mCherry:KanMX4, ura3::CFP-TUB1:URA3, BIK1-3xGFP:hphNT1</i>
<i>SPC42-mCherry:KanMX4, ura3::CFP-TUB1:URA3, BIK1-3xGFP:hphNT1, myo2-16</i>
<i>BIK1-3xGFP:hphNT1, SPC72-yeGFP:HIS3MX6</i>
<i>BIK1-3xGFP:hphNT1, SPC72-yeGFP:HIS3MX6, myo2-16</i>
<i>SPC97-mNeongreen (mNgr)</i>
<b>15DaubA</b>
<i>SPC72-sfGFP:KanMX4</i>
<i>swe1::hphNT1, SPC42-mCherry:NatNT2, ura3::CFP-TUB1:URA3</i>
<i>kin3::hphNT1, SPC42-mCherry:NatNT2, ura3::CFP-TUB1:URA3</i>

## Supplemental Experimental Procedures

### Measurement of the point spread function (PSF)

Glass slides and cover-glass was washed in 3 steps: 1) water, 2) 100 % ethanol and 3) 100 % acetone. Tetraspeck Microspheres (0.1  $\mu$ m, ThermoFisher T7279) were diluted 1:500 in 100 % ethanol. Suspended microspheres (6  $\mu$ L) were placed on the cleaned cover-glass and sealed to the glass slide using nail polish. A z-stack of 81 images was acquired at 100 nm per slice. Each bead was fit to a 3D Gaussian using non-linear regression. The PSF was obtained from the  $\sigma$  parameters that describe a Gaussian distribution.

### Simulation method used for semi-quantitative dSTORM measurements of $\gamma$ -TuC components

We simulated the exchanges between dark and bright states using a simplified kinetic model (Figure 3C). Given our short imaging regime, we assume that the fluorophore comes out and reenters the long-lived dark state once, corresponding to the inactive and bleached states. To simplify the model, the Off state was modeled as a single state as the critical step is the formation of the Alexa647-RS<sup>1</sup>[S1]. We modeled the exit from the first long dark state simply as the time to the first blink event and assume that there would not be a second round of blinking (Figure S1A, S2A).  $k_{\text{off}}$  was calculated from the distribution of the ON time (Figure S1B, S2B).  $k_{\text{on}}$  was calculated from the distribution of time between blink events (Figure S1C, S2C).  $k_{\text{bleached}}$  was calculated from the distribution of the number of blink events before it could no longer be detected (Figure S1D, S2D).

To simulate raw camera frames, we divided the photophysical traces in to camera frames according to the exposure time (20 msec.). We then simulated the number of photons being emitted based on the photon flux and the lifetime of the ON-state. Photon flux was derived from the number of photons emitted per cycle. Photon-counting noise was simulated, but EMCCD noise was not added. The simulated camera frames were analyzed as described above (see Methods).

For each  $\gamma$ -TuC simulated, the number of blink events and the width of the reconstructed were recorded. Using these parameters, we discretized the spatial distribution of the recorded super resolution spots according to the expected width of a  $\gamma$ -TuC (84 nm). For each discretized area, we calculated the cumulative probability of having at least one complete  $\gamma$ -TuC (7 for Spc97 ( $45 \pm 19$ ); 14 for Tub4 ( $82 \pm 30$ )). For the outer plaque, the highest probability bin was used. For the inner plaque, the probability was summed up across all bins.

## Supplemental References

1. Dempsey, G.T., Bates, M., Kowtoniuk, W.E., Liu, D.R., Tsien, R.Y., and Zhuang, X. (2009). Photoswitching mechanism of cyanine dyes. *J Am Chem Soc* *131*, 18192-18193.